

Performance Modeling for Dense Linear Algebra

Elmar Peise and Paolo Bientinesi
 AICES, RWTH Aachen
 Schinkelstr. 2
 52062 Aachen, Germany
 {peise,pauldj}@aices.rwth-aachen.de

Abstract—It is well known that the behavior of dense linear algebra algorithms is greatly influenced by factors like target architecture, underlying libraries and even problem size; because of this, the accurate prediction of their performance is a real challenge. In this article, we are not interested in creating accurate models for a given algorithm, but in correctly ranking a set of equivalent algorithms according to their performance. Aware of the hierarchical structure of dense linear algebra routines, we approach the problem by developing a framework for the automatic generation of statistical performance models for BLAS and LAPACK libraries. This allows us to obtain predictions through evaluating and combining such models. We demonstrate that our approach is successful in both single- and multi-core environments, not only in the ranking of algorithms but also in tuning their parameters.

I. INTRODUCTION

For a large class of dense linear algebra operations, such as the solution of least squares problems and linear systems, not one but many algorithms exist. While mathematically they are equivalent, their performance depends—in different ways—on factors such as the target architecture, the underlying libraries, and the problem size. The prediction of the best performing algorithm in a given scenario is a challenging task. Our goal is to *rank the algorithms* according to their performance and to determine their optimal configuration *without executing them*.

As a motivating example, we consider the inversion of a lower triangular matrix ($L \leftarrow L^{-1}$), for which there exist four blocked algorithms, all equivalent in exact arithmetic, but with different performance signatures. Each such algorithmic variant depends on one parameter, the block-size b , which determines the stride in which the matrix is traversed.

In Figure I.1 we plot their efficiency—the relative measure of the machines resource utilization—when executed on one core of an Intel Harpertown E5450;¹ the block-size is fixed to 96 and the matrix size n varies. The results show noticeable differences in performance between algorithms: Variant 4 (●) is significantly slower than the others, while, especially for large matrices, variant 3 (●) is the most efficient. In Figure I.2, we fix $n = 1000$ and let b vary; in all variants, the efficiency decreases for small and large block-sizes. For variants 1 (●), 2 (●), and 3 (●) the optimal choice of b is close to 100.

This example shows that in order to reach high efficiency, it is crucial to both single out the right algorithmic variant,

¹ The algorithms were implemented in C, compiled with ICC version 12.0, and linked to Intel’s MKL version 10.2.6. In all cases, our algorithms use library calls to perform calculations; because of this, compiler’s optimizations do not influence the resulting performance.

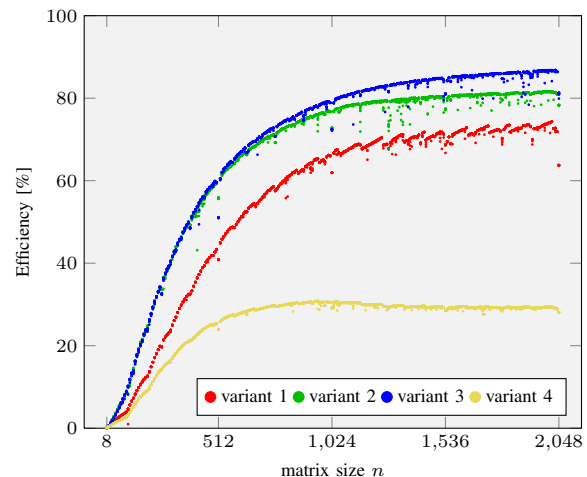


Fig. I.1: Inversion of a lower triangular matrix: Efficiency as a function of the problem size.

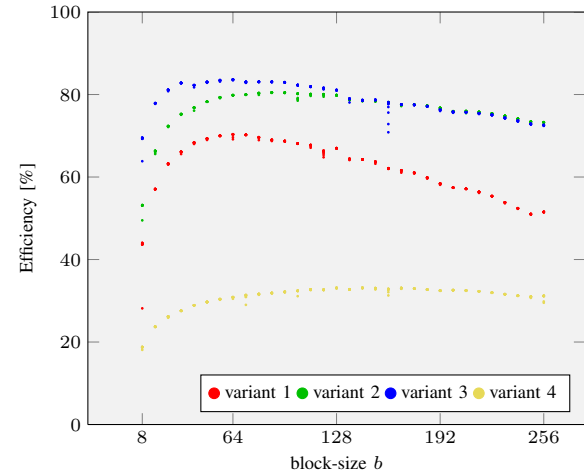


Fig. I.2: Inversion of a lower triangular matrix: Efficiency as a function of the block-size.

and optimize the block-size. Due to the complexity of the architecture and the memory access patterns, it is virtually impossible to perform these tasks only by analyzing the mathematics of the algorithms. Indeed, experience tells us that the best choice heavily depends on the computational kernels used, such as BLAS, on the processor architecture, and the matrix size; changing any of these factors may lead to entirely different performance behavior.

In this article, we detail a strategy based on the analysis of the BLAS routines upon which the target algorithms are

built; we introduce a tool that, using measurements, creates performance models for BLAS kernels and stores them permanently in a repository. When faced with a set of algorithms, the models are evaluated and combined to predict the algorithms’ performance. These predictions allow us not only to accurately rank the algorithmic variants, but also to determine the optimal algorithmic block-size.

Several different approaches to performance modeling in dense linear algebra exist; some notable examples are given in the following. Cuenca et al. developed a system of self-optimizing linear algebra routines (SOLAR) [1]; every routine is associated with performance information, which is hierarchically propagated to higher level routines in order to tune them. Dongarra et al. proposed an approach for parallel software such as HPL and ScaLAPACK [2]; they employ sampling and polynomial fitting to construct models in order to extrapolate the performance of routines for larger problems and higher parallelism. Dackland et al. predict the performance of ScaLAPACK algorithms through models based on the efficiency of BLAS and the time spent on communication [3]. Balaprakash et al. apply mathematical optimization techniques to reduce the number of measurements in empirical performance tuning [4]. Iakymchuk et al. model the performance of BLAS analytically based on memory access patterns [5]; while their models represent the program execution very accurately, constructing them requires a high level of expertise of both routines and architecture.

In contrast to the aforementioned approaches, we aim at the automatic generation of accurate models for BLAS routines, which constitute the building blocks of a multitude of algorithms in linear algebra. Our main goal is not to obtain accurate prediction for these algorithms, but rather to correctly rank them and tune their configuration.

This article is structured as follows. In Section II, we discuss the performance of dense linear algebra routines. In Section III, we introduce the *Modeler*, a tool that automatically generates analytical performance models. Predictions and ranking are discussed in Section IV, and in Section V we draw conclusions.

II. PERFORMANCE

In this section, we discuss the concept of performance in the context of dense linear algebra, and introduce *the Sampler*, a performance measurement tool for linear algebra routines.

A. Performance Metrics

In the following, the term performance is used broadly to cover a set of *performance metrics* that describe certain aspects of a routine execution, such as timings, instruction counts, and cache accesses. The metrics are either directly obtained from hardware performance counters or are quantities computed from them. The most fundamental performance counter — the time stamp counter — is provided by a register that is incremented once per CPU cycle. It is accessed through the x86 instruction RDTSC and serves as a cycle-accurate timer; we refer to this metric as *ticks*. In order to access more CPU performance counters, we use the Performance Application

[[IMAGE DISCARDED DUE TO '\tikz/external/mode=list and make']]

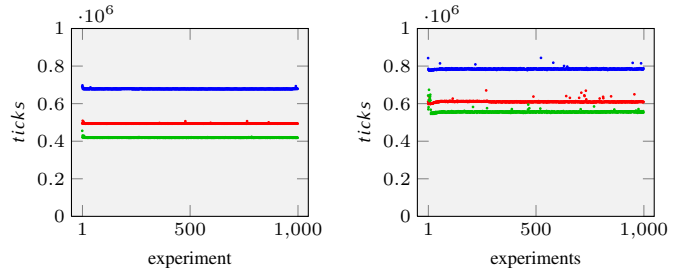


Fig. II.1: Repeated execution of `dtrsm`: In-cache (left) and out-of-cache (right) operands.

Programming Interface (PAPI) [6]². PAPI provides functions to configure, initialize, and read up to 107 counters, but usually only a subset of which are available in a given system.

In this article we focus on the highly accurate time metric *ticks*. In additions, we use the derived metric *efficiency*, representing the relative resource utilization:

$$efficiency = \frac{flops}{ticks \cdot fips}.$$

This measures how efficiently an operation that performs *flops* floating point instructions³ uses the CPU’s ALUs, which can perform up to *fips* floating point instructions per cycle.

B. Performance of dense linear algebra routines

At this point, we are interested in the performance of dense linear algebra routines, such as BLAS or unblocked algorithms, that act as building blocks for higher level algorithms. Our first objective is to build performance models for such building blocks.

For a given architecture, we regard the performance of a routine as a function of the arguments. Apart from the buffers for matrices and vectors, all the arguments are simple to represent in such a function, since they are basic data types such as characters, integers, and floating point numbers. Since the instructions performed by the dense linear algebra routines we consider are mostly independent of the input data, we can reduce the information needed for these arguments to their size and storage location in the memory hierarchy.

Regarding memory locality, we distinguish two cases: in-cache and out-of-cache. *In-cache* refers to the situation where all matrices are as close to the CPU as possible, that is, in the lowest cache level that can accommodate them. Since the access time is minimized, this scenario leads to the best performance the routine can attain. *Out-of-cache* refers to the opposite situation, where the matrices reside in main memory, thus causing costly data transfers. Since the loading and storing of data might result in memory stalls, the overall performance is often inferior than when data resides in cache.

To study the influence of memory locality and the reproducibility of measurements, let us consider a repeated

²PAPI version 4.2.1.0.

³A fused multiply add operation $a \leftarrow b + c \cdot d$ is counted as a single floating point operation, since it is one instruction and processed as such by the CPU.

execution of the BLAS routine `dtrsm` ($B \leftarrow A^{-1}B$, A triangular). The interface is

```
dtrsm( R , L , N , U , 512 , 128 ,
      alpha , A , ldA , B , ldB ,
      0.37 , A , 256 , B , 512 ) ,
```

corresponding to the operation $B \leftarrow 0.37BA^{-1}$, where $A \in \mathbb{R}^{128 \times 128}$ is lower triangular with leading dimension $\text{ldA} = 256$, and $B \in \mathbb{R}^{512 \times 128}$ with $\text{ldB} = 512$. In our experiment, this operation is repeatedly executed on one core of our Harpertown, using the high-performance BLAS implementations OpenBLAS, MKL, and ATLAS⁴. Notice that the first invocation of a BLAS routine is always notably (in our case more than one order of magnitude) slower than the following one, due to the initialization of BLAS, which happens at the first invocation of the library. Neglecting these first measurement outliers, the performance measurements of the routine executions with both in-cache and out-of-cache arguments are shown in Figure II.1. As expected, in-cache corresponds to higher performance across all implementations, while the increase in execution time for out-of-cache varies from one implementation to the other. In our study—in which the performance of algorithms is obtained through models of the algorithms’ components—memory locality will play a big role.

In addition to the influence of memory locality, we observe fluctuations in the performance measurements of about 8%. For this reason, we do not consider the routine’s performance to be one number but a probabilistic distribution. To express the performance in numbers, we select certain properties of this distribution, such as minimum, average, standard deviation, and median.

C. The Sampler

To facilitate the acquisition of performance measurements, we wrote the Sampler, a flexible lightweight performance measurement tool. Written in C, the Sampler directly interfaces with libraries such as BLAS or LAPACK. Its configuration allows to choose between different memory locality situations. Given routine names and arguments in the form of tuples, such as $(\text{dtrsm}, R, L, N, U, 512, 128, 0.37, A, 256, B, 512)$ (A and B specify the sizes of the operands), the Sampler measures and reports the performance of the routines; this entails collecting multiple samples and extracting statistical information.

III. MODELING

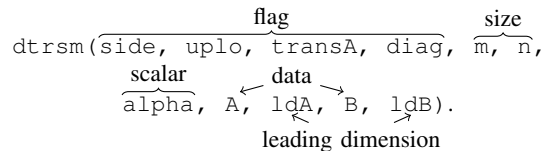
With the measurements obtained by the Sampler, we want now to construct analytical performance models. Here we introduce the *Modeler*, a tool which interacts with the Sampler and automatically generates performance models. These models form the base for the performance prediction and algorithm ranking (Section IV).

⁴ BLAS provides us with the necessary kernels used in the calculations; we do not attempt any optimization of such routines.

A. Preliminary Experiments

Most BLAS routines accept 10 or more arguments; LAPACK’s routines have easily twice as many. In building performance models, if we blindly treated all the arguments equally, we would originate 10+ dimensional models, which would result in either impractical execution times or sloppy accuracy. To avoid this curse of dimensionality, we analyze how different arguments types affect performance, and in our models we only account for a subset of the arguments.

Here we focus on the dependence of performance on the BLAS arguments. Again, we use `dtrsm` as an example; the arguments of BLAS routines can be classified as follows:



Flag arguments take one of only two values (e.g., $\text{side} \in \{\text{L}, \text{R}\}$); *size* arguments contain the dimensions of the matrix and vector operands; *scalars* are floating point numbers, which scale the operands; *data* are (pointers to) the buffers in which the operands are stored; *leading dimensions* define the distance in memory between two horizontally adjacent matrix entries.

Due to the following reasons, for our purposes we can disregard all but flag and size arguments.

- Scalar arguments are usually set to 1 or -1 . Neither of these values requires any floating point operations to perform the scaling, thus not affecting performance. Even other values for scalar arguments have an insignificant influence on performance, since they only affect a lower order term of the operation count.
- As discussed in Section II-B, only the size and storage location of vector and matrix arguments are relevant for performance. The sizes of these operands are covered by the size and leading dimension arguments. As for the storage locations, we will construct separate models for different memory locality scenarios, so that we can entirely ignore data arguments within one model.
- In practice, the leading dimensions are either equal to the size of a corresponding input matrix or larger. While the difference between these two scenarios can influence performance, we only need to consider the latter: within our targeted algorithms, the BLAS routines are invoked on parts of a large input matrix of constant dimension. Hence, throughout the model generation, all leading dimension arguments are set to 2500.

Next, we study the influence of the flags and the size arguments on the performance of BLAS routines.

1) *Flag Arguments*: All types of flag arguments encountered in BLAS appear in the signature of `dtrsm`: $\text{side} \in \{\text{L}, \text{R}\}$ defines from which side B is multiplied by A^{-1} ; $\text{uplo} \in \{\text{L}, \text{U}\}$ states if A is lower or upper triangular; $\text{transA} \in \{\text{N}, \text{T}\}$ indicates whether A or its transpose A^T is to be used; when set to U , $\text{diag} \in \{\text{N}, \text{U}\}$ declares that A is unit triangular.

In Figure III.1, we report on a series of experiments in which

rameters.⁵

Each submodel is essentially a vector-valued multivariate piecewise polynomial in the following sense. The integer parameters span a multidimensional space, which is covered by rectangular regions, in which the behavior is represented by polynomials. Each polynomial is vector valued with one value for each statistical quantity.

When the model is used to estimate the performance for given routine arguments, the following happens: (1) the model parameters are extracted; (2) the submodel corresponding to the combination of flags is identified; (3) the region containing the integer parameter point is found; (4) the polynomial corresponding to the region is evaluated, yielding the estimates.

C. The Modeler

In the previous section, we have described the structure of our targeted performance models. We now introduce the Modeler, a tool that generates these models automatically.

We skip the technicalities that arise from creating a separate model for each combination of flags and instead focus on the generation of piecewise polynomials to model the dependence of performance on integer parameters. The objective of the Modeler is to attain accuracy automatically and with as few measurements as possible. Moreover, although within BLAS at most three integer parameters are encountered, the Modeler is designed for arbitrary dimension.

Polynomial Fitting through Least Squares: The approximation of a set of sampling results by polynomials through least squares fitting is a fundamental task of the modeling process. A set of n coordinate value pairs (\mathbf{x}_i, v_i) are fitted with a polynomial p of limited order, such that

$$\sum_{i=1}^n (p(\mathbf{x}_i) - v_i)^2$$

is minimized. To solve this least squares problem, we use the function `linalg.lstsq()` provided by Python's SciPy package, which is based on singular value decomposition.

The accuracy of a polynomial approximation p is determined by the local errors $e_i = p(\mathbf{x}_i) - v_i$. While the used least squares method minimizes $\sum_{i=1}^n e_i^2$, we use the *maximum relative error* across all \mathbf{x}_i :

$$e_{\text{relmax}} = \max_{1 \leq i \leq n} \frac{|e_i|}{v_i}.$$

To create the vector valued polynomial for the statistical quantities, each quantity is separately fitted with a polynomial. The error e_{relmax} of one quantity is picked to represent the accuracy of the whole polynomial. In the following, we use the median for this purpose.

1) *Model Expansion:* We now introduce the first of two modeling strategies, *Model Expansion*. The piecewise polynomial is created according to the following steps.

- The first objective is to build a model for a small region in a corner of the parameter space; this is accomplished by fitting a small set of measurements.

⁵Since there are no more than 4 flag arguments in BLAS routines, the number of submodels stays well within manageable bounds.

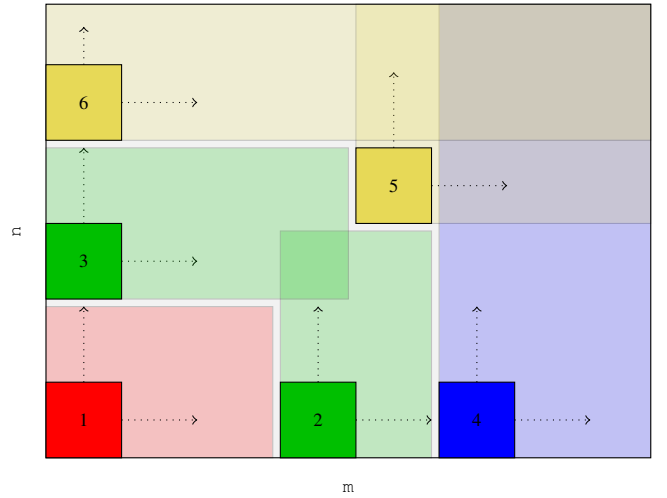


Fig. III.4: Sequence of steps in the construction of piecewise models through Model Expansion.

- This initial region is then expanded as much as possible, by taking new measurements, integrating them in the model, and checking that
 - a) the polynomial's approximation error is below a given threshold, and
 - b) the region stays within the boundaries of the parameter space.
- Once a region cannot be extended further —because of either a) or b)— new adjacent regions are generated and expanded.

The process is repeated until the whole parameter space is covered.

An example of Model Expansion in two dimensions is given in Figure III.4. The rectangular domain is filled starting with region 1 (red) in the bottom-left corner of the domain. This region is expanded in both directions until its accuracy reaches the threshold (pink). Two new adjacent regions 2 and 3 (green) are then created —together with the associated samples— and their expansion begins. Assuming that region 2 was expanded as far as possible (light green), region 4 (blue) is then generated. Once the expansion for region 3 (green) is complete, the neighboring regions 5 and 6 (yellow) are created. These 6 models cover the full parameter space, therefore the process terminates.

2) *Adaptive Refinement:* The second strategy to generate piecewise models is based on adaptive refinement. The idea is to begin with a simple and regular model constructed from a coarse grid of samples across the whole parameter space; the quality of such a model is then evaluated. If insufficient, the region is split and the model is refined by locally increasing the sample grid resolution. These steps are applied recursively to the refined regions until either the accuracy reaches a satisfactory level across the whole domain, or a given resolution limit is reached.

An example of Adaptive Refinement for a two dimensional domain is shown in Figure III.5. The polynomial approximation for the initial region spanning the entire parameter space is very inaccurate (red, 1st square on the left). Therefore it is refined, generating four new regions, and new measurements

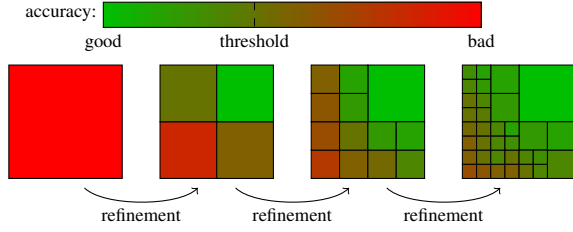


Fig. III.5: Sequence of steps in the construction of piecewise models through Adaptive Refinement.

are obtained to create four polynomials (2^{nd} square on the left). Now, the error in the top right quadrant (■) is already below the threshold (■); the other quadrants are not accurate enough and are further refined (3^{rd} square). In the next iteration, several regions are below the desired error threshold; the others are refined once more (4^{th} square). Although some of the resulting polynomials are still above the desired level of accuracy, they are accepted anyway, because their size does not allow further refinement.

D. Results

Having introduced two modeling strategies, here we compare the resulting models, both in terms of speed and accuracy. We consider again the solution of a triangular system $B \leftarrow A^{-1}B$ as testbed:

```
dtrsm(side, uplo, transA, diag, side, m, n,
      alpha, A, ldA, B, ldB).
```

The interface of this routine contains four flags (*side* through *diag*), two size arguments (*m* and *n*), one scalar argument (*alpha*), and operates on two matrices (*A* and *B* with corresponding leading dimensions *ldA* and *ldB*). Out of these arguments, our models account for

- the flag parameters *side*, *uplo*, and *transA*, and
- the integer parameters *m* and *n*.

The integer parameters vary in the range $[8 - 1024]$ and define the parameter space; the flags are $(\text{side}, \text{uplo}, \text{transA}) = (\text{L}, \text{L}, \text{N})$; the values of the remaining arguments are: *diag* = *N*, *alpha* = 0.5, and *ldA* = *ldB* = 2500. We use the in-cache configuration of the Sampler and OpenBLAS on the Harpertown processor.

1) *Model Expansion*: This approach accepts several configuration options:

- the relative error bound ε ;
- the direction of expansion $d \in \{\nearrow, \swarrow\}$;
- the initial size of regions s_{ini} .

We illustrate the influence of such options on the generation by presenting models obtained with different settings. The plots in Figure III.6 show how differently these models cover the parameter space and display the relative errors.

In Figure III.6a, we used the configuration:

- the error bound is $\varepsilon = 10\%$;
- the direction of expansion is $d = \nearrow$;
- new regions are initially of size $s_{ini} = 64$.

Smaller and less accurately modeled regions are generated towards the left side of the parameter space. Towards the top

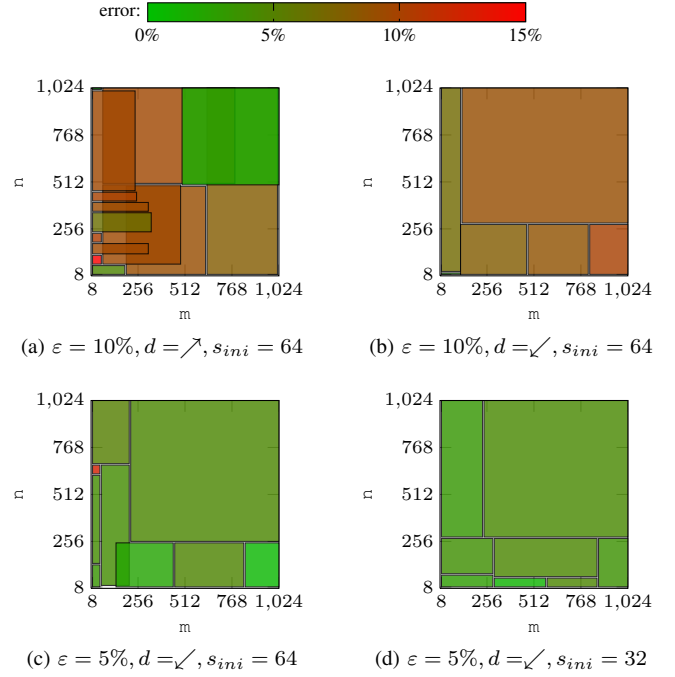


Fig. III.6: Model Expansion for *dt_rsm*.

right corner, the regions become larger and the relative error decreases. In this part of the parameter space, we also find several areas which are modeled by two or more overlapping regions⁶.

In Figure III.6b instead, we let the Modeler expand along the direction $d = \swarrow$. We observe the following changes:

- especially towards the top right corner, the generated regions are larger;
- these regions are of higher accuracy compared to the previous model, although the error bound was not modified;
- fewer regions overlap.

The average relative error improves from 8.26% to 7.77%, while the number of required sampling points decreases from 5280 to 2070. We noticed that in general, it is preferable to expand the models towards the origin (\swarrow).

In Figure III.6c, we reduced the error bound to $\varepsilon = 5\%$. As a result, the average model error improves from 7.77% to 3.87%. This comes at the cost of an increase in the number of samples: from 2070 to 2990. As in the previous cases, the accuracy of the models decreases as the parameter values become smaller; the least accurate models appear for small values of *m*.

Finally, in Figure III.6d we decreased the size of the initial models from $s = 64$ to $s = 32$. Interestingly, even though the model now makes use of only 2710 samples, the average error decreases from 3.87% to 3.80%. This is due to the fact that the sample points are shifted, and irregularities present in the previous models are not captured. From this we conclude that an index of accuracy generated from used samples is not always sufficient to capture the global quality of a model.

2) *Adaptive Refinement*: The generation of models is governed by two options:

⁶When the model is evaluated at a point covered by multiple regions, the most accurate model is selected.

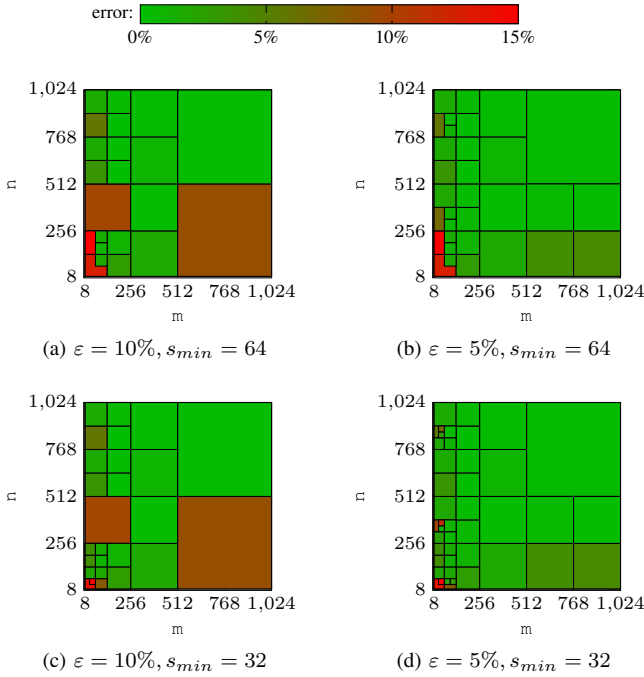


Fig. III.7: Adaptive Refinement for dt rsm.

- the relative error bound ε , and
- the minimum region size s_{min} .

The regions resulting from different values of these options are shown in Figure III.7.

The first model in Figure III.7a was generated with an error bound of $\varepsilon = 10\%$ and a minimum region size of $s = 64$. The result shows an overall distribution of regions similar to the model in Figure III.6d of Model Expansion: Smaller and less accurately modeled regions are predominant for smaller parameter values — especially for m . Regions on the finest level are not generated on the lower edges of the parameter space (beginning at 8), since they would be smaller than s_{min} . The seemingly rectangular regions are parts of larger regions that were only partially refined.

In Figure III.7b, the error bound was decreased to $\varepsilon = 5\%$. For such an accuracy to be attained, several of the regions from the previous model are further refined, especially on the left side. The increased number of regions is covered by 3560 samples — 970 more than previously. The higher accuracy requirement leads to a decrease in the average error from 7.17% to 2.41%.

In the next two experiments, Figures III.7c and III.7d, we decreased the minimum region size to $s = 32$, maintaining the error bound ε to 10% and 5%, respectively. This leads to the generation of many tiny regions. The error bound of 10% (5%) leads to an average error of 6.20% (1.45%) at the cost of 3070 (4980) samples.

3) *Comparison*: Figure III.8 displays, for both modeling strategies, how many samples are needed to generate models of a certain accuracy. The models presented in the previous sections are labeled according to Figures III.6 and III.7. We are interested in models that attain a high degree of accuracy with a small number of samples; these are the points laying

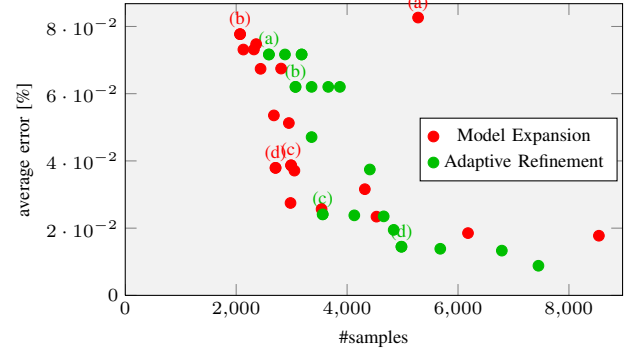


Fig. III.8: Model Expansion vs. Adaptive Refinement.

in the bottom left border of the convex hull (envelope) of all the points.

For relatively few samples, Model Expansion generates more accurate models ((b) and (d)). However, one should keep in mind that these models do not necessarily represent the fine scale behavior of *ticks* very well. If one is willing to use a larger number of samples, Adaptive Refinement generates more accurate models ((c)). If the number of samples is not an issue, this method has the potential to generate very accurate models ((d)).

In the experiments performed in the rest of the paper, we used Adaptive Refinement with configuration (c): $\varepsilon = 10\%$ error bound and $s_{min} = 32$ minimum regions size. This configuration is a good compromise between the model accuracy and the number of samples.

IV. PREDICTION, RANKING AND OPTIMIZATION

We are finally ready to tackle our main goal: ranking linear algebra algorithms by performance models. In order to predict the performance of an algorithm, we start by analyzing its sequence of subroutine invocations. We use the models automatically generated by the Modeler to estimate the performance of such invocations. These estimates are then accumulated, resulting in the prediction of the algorithm's performance. The probabilistic nature of the performance model allows us to give detailed information on the expected ranges of the algorithm's performance.

A. Triangular Inverse $L \leftarrow L^{-1}$

We consider four blocked algorithms for the inversion of a triangular matrix. All these algorithms partition L into 6 submatrices as

$$L = \begin{pmatrix} L_{00} & 0 & 0 \\ L_{10} & L_{11} & 0 \\ L_{20} & L_{21} & L_{22} \end{pmatrix}.$$

The central matrix L_{11} is of size $b \times b$ (the block-size); the size of the matrix L_{00} is initially 0×0 , and as the algorithm unfolds, it increases in steps of size b , until L_{00} spans the whole matrix L ; the size of L_{22} decreases accordingly; similarly, the sizes of the offdiagonal matrices are entirely determined by those of L_{00} . At each step of this matrix traversal, a sequence of update statements is performed on the submatrices, such that

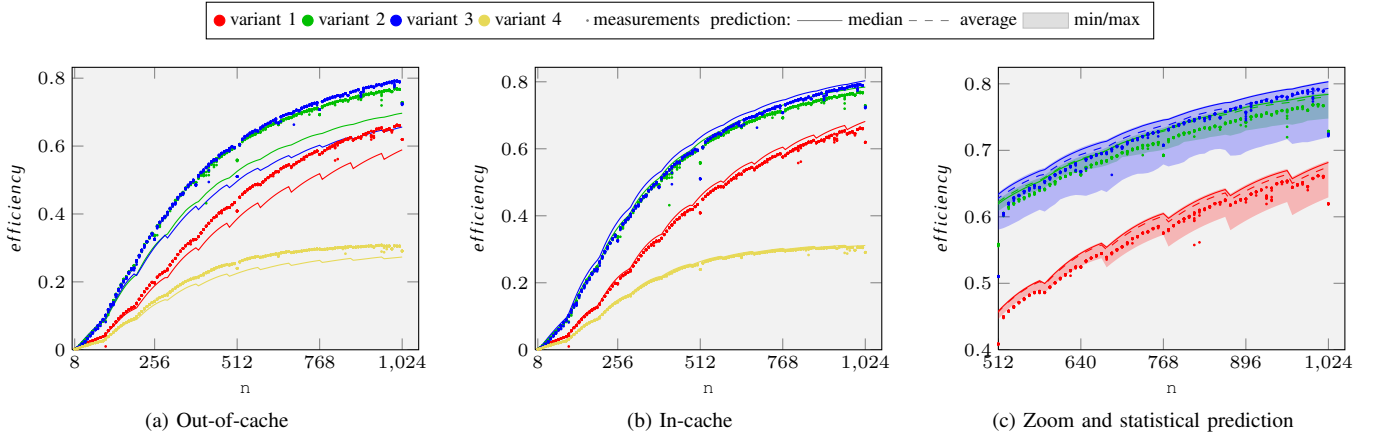


Fig. IV.1: `trinv`: Performance predictions vs. observations.

L_{00} contains a fully computed portion of L^{-1} . Once L_{00} spans all of L , L^{-1} has been computed in place.

The four algorithmic variants presented here differ in their update statements:

Variant 1	Variant 2
$L_{10} \leftarrow L_{10}L_{00}$	$L_{21} \leftarrow L_{22}^{-1}L_{21}$
$L_{10} \leftarrow -L_{11}^{-1}L_{10}$	$L_{21} \leftarrow -L_{21}L_{11}^{-1}$
$L_{11} \leftarrow L_{11}^{-1}$	$L_{11} \leftarrow L_{11}^{-1}$
Variant 3	Variant 4
$L_{21} \leftarrow -L_{21}L_{11}^{-1}$	$L_{21} \leftarrow -L_{22}^{-1}L_{21}$
$L_{20} \leftarrow L_{21}L_{10} + L_{20}$	$L_{20} \leftarrow -L_{21}L_{10} + L_{20}$
$L_{10} \leftarrow L_{11}^{-1}L_{10}$	$L_{10} \leftarrow L_{10}L_{00}$
$L_{11} \leftarrow L_{11}^{-1}$	$L_{11} \leftarrow L_{11}^{-1}$

They are built on top of the BLAS routines `dgemm`, `dtrsm`, and `dtrmm`; the last statement in each algorithm is a recursive call to an unblocked version of the same algorithm. They have the following signatures: `trinv(n, L, ldL, blocksize)`. We consider their performance with the arguments

$$\text{trinv}(n, L, n, 96),$$

varying the matrix size $n \in \{8, 16, \dots, 1024\}$. We consider the performance metric *efficiency*, which is computed from *ticks* as follows:

$$\text{efficiency} = \frac{\frac{1}{6}n^3 + \frac{1}{2}n^2 + \frac{1}{3}n}{2 \cdot \text{ticks}}.$$

For our performance prediction, we use performance models for `dtrsm`, `dtrmm`, `dgemm`, and the unblocked versions of the blocked algorithms⁷. The models are generated by the Modeler, with the configuration selected in Section III-D3. For each algorithm execution, we consider the list of subroutine invocations, consisting of calls to these routines. For instance, the execution of variant 1 on a matrix of size 250 with block-size 100 produces the following invocations:

```
dtrmm(R, L, N, N, 100, 0, 1, L00, 250, L10, 250)
dtrsm(L, L, N, N, 100, 0, -1, L11, 250, L10, 250)
```

⁷Since the unblocked versions are only invoked on small matrices, their models are limited to values of n below 256.

```
trinv1(100, L11, 250, 1)
dtrmm(R, L, N, N, 100, 100, 1, L00, 250, L10, 250)
dtrsm(L, L, N, N, 100, 100, -1, L11, 250, L10, 250)
trinv1(100, L11, 250, 1)
dtrmm(R, L, N, N, 50, 200, 1, L00, 250, L10, 250)
dtrsm(L, L, N, N, 50, 200, -1, L11, 250, L10, 250)
trinv1(50, L11, 250, 1).
```

Each invocation corresponds to the evaluation of the corresponding performance model; the results are then accumulated, thus generating a performance prediction.

1) *Matrix size*: Figure IV.1 contains the predictions for the four algorithm, with varying matrix size. The left and middle panels refer to in-cache (IV.1b) and out-of-cache (IV.1a) scenarios, respectively. Since the memory locality of an actual execution is somewhere in between these two scenarios, neither of the predictions matches the measurements perfectly: in-cache overestimates the efficiency of the algorithms, while out-of-cache underestimates it. At this moment we do not yet attempt the construction of models matching the exact memory locality scenario of each algorithm; therefore in the following we use the upper bound on efficiency resulting from the in-cache models. This prediction ranks exactly all variants for all problem sizes.

The previous discussion referred to predictions for the median of the performance. In Figure IV.1c we instead look at average, minimum, and maximum efficiency; in order to visualize the interesting features, we only present the top right portion of the graph ($n \geq 512$ and $0.5 \leq \text{efficiency} \leq 0.8$). The ranges between minimum and maximum (shaded area) cover almost all the observations of the corresponding algorithms, giving a good idea of the expected results; their height is due to the presence of outliers.

The average (dashed line) is closer to the measured algorithm performance than the previously used median. Nevertheless, relying on the average predictions, is dangerous, since they are obtained for models generated with an error bound on the median and are influenced by outliers.

Altogether, we predicted performance for varying matrix sizes with highly satisfactory results.

2) *Block-size*: We now turn our attention to our second point of interest: tuning the block-size to yield the best

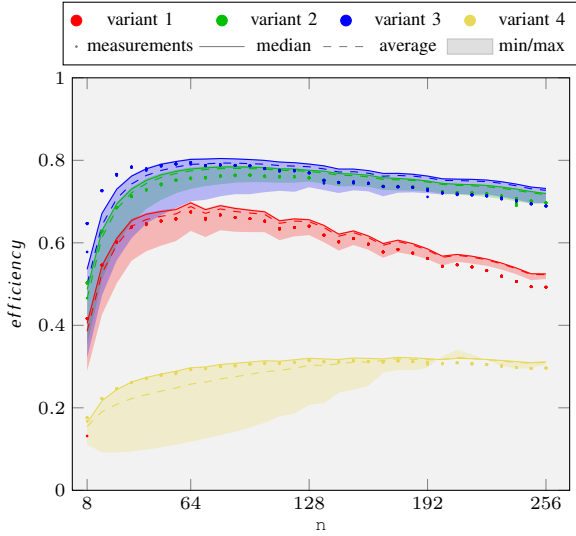


Fig. IV.2: Block-size optimization for `trinv`.

efficiency. For this purpose, we fix the matrix size to $n = 1000$ and vary the block-size:

```
trinv(n, L, ldL, blocksize)
trinv(1000, L, 1000, blocksize).
```

The resulting predictions (Figure IV.2) capture very well the behavior for the most efficient block-sizes (between 48 and 128). For instance, Variant 3 (●) —the fastest— attains its top performance with a block-size of 64 according to both the measurements and our prediction.

The quality of our prediction decreases for very large and very small block-sizes. For our goal —determining the fastest algorithm configuration— the low accuracy in regions with low performance is not an issue. The decreasing accuracy in the maximum and average performance for variant 4 (●), resulting from measurement outliers in the model generation, shows that these quantities are less well suited for predictions. The median on the other hand is very reliable.

3) *Sandy Bridge*: We now move to a newer CPU architecture: Intel’s Sandy Bridge-EP E5-2670 running at 2.60GHz. On this system, we use the OpenBLAS library, for which we generate a new set of performance models. The predictions for `trinv` obtained from these models are shown in Figure IV.3. As for the Harpertown, the least efficient variant is #4 (●); however, on this system the fastest variant is #1 (●). Besides, while on this processor the predictions for some variants are not as accurate as on the Harpertown, the ranking is still carried out correctly.

4) *Shared memory parallelism*: Our modeling strategy applies well to shared memory architectures too. In this next experiment, we utilize all the 8 cores of the Sandy Bridge processor. We achieve parallelism by linking the routines for matrix inversions with the multithreaded version of the OpenBLAS library. The performance predictions are obtained from performance models generated from measurements of the multithreaded BLAS routines.

The resulting predictions along with measurements of `trinv`’s performance are shown in Figure IV.4. The pre-

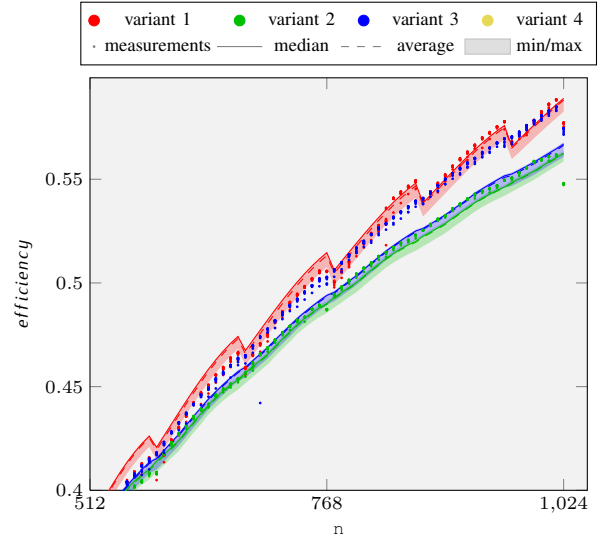


Fig. IV.3: `trinv`: Predictions and observations on Sandy Bridge.

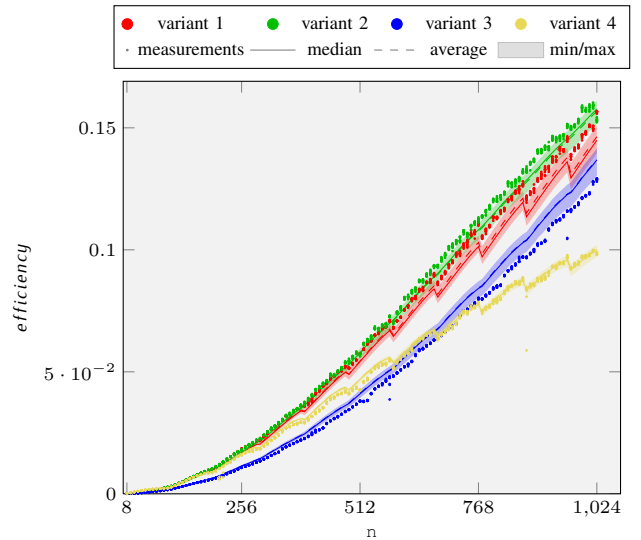


Fig. IV.4: `trinv`: Predictions and observations on 8 cores.

dictions match the experiments very closely and allow us to rank the algorithmic variants correctly for all problem sizes. Moreover, the multithreaded variants exhibit two interesting features: At about $n = 650$, variants 3 (●) and 4 (●) crossover, and in contrast to the sequential case, variants 1 (●) and 2 (●) are faster than variant 3 (●). Both these features also appear in our predictions.

B. Sylvester Equation: Solving $LX + XU = C$ for X

We now study of a more complicated operation: the solution of the Sylvester equation. This operation, encountered in control theory, is generally of the form $AX + XB = C$, where $A \in \mathbb{R}^{m \times m}$, $B \in \mathbb{R}^{n \times n}$, and $C \in \mathbb{R}^{m \times n}$ are given, and $X \in \mathbb{R}^{m \times n}$ is to be computed. We consider a special case, where A and B are lower and upper triangular matrices, respectively: $LX + XU = C$.

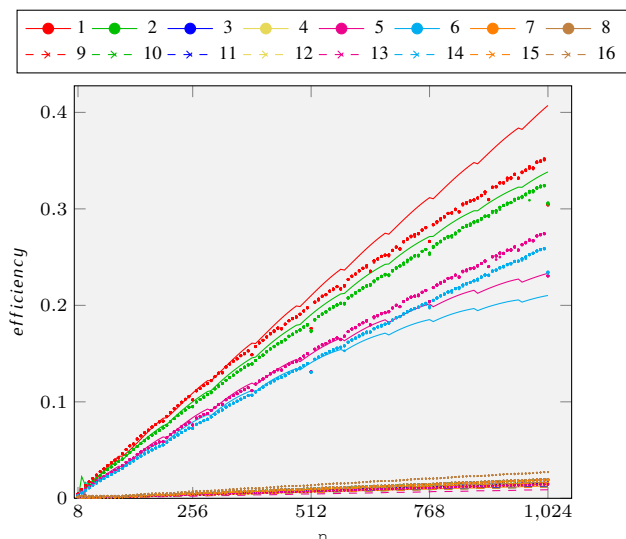


Fig. IV.5: `sylv`: Predictions (—) vs. observations (•, ×).

With `CLICK` [7], [8], a tool for the automatic generation of blocked algorithms, we generated code for 16 algorithmic variants. Each of them takes as input the three matrices L , U , and X ; X initially contains the input matrix C and is overwritten with the solution to the equation.

The exemplary update statements for variants 1 and 16 are given below. There, $\Omega(L, U, X_{ij})$ denotes a recursive invocation to the Sylvester equations solver for the smaller matrix X_{ij} . The signature of this solver is `sylvi(m, n, L, ldL, U, ldU, X, ldX, blocksize)` with $i \in \{1, \dots, 16\}$.

Variant 1	Variant 16
$X_{01} \leftarrow X_{01} - X_{00}U_{01}$	$X_{11} \leftarrow \Omega(L_{11}, U_{11}, X_{11})$
$X_{10} \leftarrow X_{10} - L_{10}X_{00}$	$X_{12} \leftarrow X_{12} - X_{11}U_{12}$
$X_{01} \leftarrow \Omega(L_{00}, U_{11}, X_{01})$	$X_{21} \leftarrow X_{21} - L_{21}X_{11}$
$X_{10} \leftarrow \Omega(L_{11}, U_{00}, X_{10})$	$X_{12} \leftarrow \Omega(L_{11}, U_{22}, X_{12})$
$X_{11} \leftarrow X_{11} - X_{10}U_{01}$	$X_{21} \leftarrow \Omega(L_{22}, U_{11}, X_{21})$
$X_{11} \leftarrow X_{11} - L_{10}X_{01}$	$X_{22} \leftarrow X_{22} - X_{21}U_{12}$
$X_{11} \leftarrow \Omega(L_{11}, U_{11}, X_{11})$	$X_{22} \leftarrow X_{22} - L_{21}X_{12}$

These blocked algorithms differ from those for `trinv` in a number of ways.

- They operate on three matrices, overwriting one of them with the output.
- The input matrices are of different sizes, and not all of them are square: $L \in \mathbb{R}^{m \times m}$, $U \in \mathbb{R}^{n \times n}$, and $X \in \mathbb{R}^{m \times n}$. Moreover, the matrices are traversed along the diagonal as far as possible and then along the remaining dimension.
- At each iteration, the algorithms perform three recursive calls to Ω . These operate not only on the $X_{11} \in \mathbb{R}^{\text{blocksize} \times \text{blocksize}}$ but also on the matrix panels X_{01} , X_{10} , X_{12} , and X_{21} . For the latter, our C implementation invokes the blocked algorithms recursively; only the small matrices X_{11} trigger their unblocked versions.

In our tests, we consider the case

```
sylvi(n, n, L, n, U, n, X, n, 96).
```

All matrices are of size $n \times n$, $n \in \{8, 16, \dots, 1024\}$ and we use 96 as block-size. Figure IV.5 compares our predictions for these algorithms with corresponding measurements of their implementations, where

$$efficiency = \frac{n^3 + n^2}{2ticks}.$$

We observe significantly different performances across algorithms: At $n = 1024$ variant 1 (—•—) is more than 20 times faster than variant 13 (—×—). Indeed, twelve of the variants attain a performance below 2%, while the other four reach values around 20%. In such a scenario, it is first crucial to tell apart the two groups, and then to correctly rank the four top variants. Although our individual predictions are not especially accurate, they fulfill the objective perfectly, separating the groups, and ordering variants 1 (—•—), 2 (—•—), 5 (—•—), and 6 (—•—) as the top most efficient algorithms.

V. CONCLUSION

In this article, we presented an approach to analyze and model the performance of dense linear algebra routines. Our goal was to rank a given collection of blocked algorithms according to their performance and to optimize their configuration, without executing them. Towards this goal, we created a performance modeling tool, the `Modeler`, that automatically generates models for BLAS and LAPACK routines. We introduced two strategies to originate piecewise polynomial models, to favor either speed or accuracy. Upon creation, the set of models is stored in an easily accessible repository, for easy access and evaluation. In order to predict the performance of a blocked algorithm, the performance models of its building blocks are then evaluated and combined.

We showed that the approach is applicable to operations with numerous algorithm variants both on single- and multi-core systems; experiments confirmed that our predictions are able to both correctly tell apart the variants according to their performance, and to identify the optimal algorithmic block-size.

REFERENCES

- [1] J. Cuenca, D. Giménez, and J. González, “Architecture of an automatically tuned linear algebra library,” *Parallel Comput.*, vol. 30, no. 2, pp. 187–210, Feb. 2004. [Online]. Available: <http://dx.doi.org/10.1016/j.parco.2003.11.002>
- [2] J. Dongarra and P. Luszczek, “Reducing the time to tune parallel dense linear algebra routines with partial execution and performance modelling,” University of Tennessee Computer Science Technical Report, Tech. Rep., 2010.
- [3] K. Dackland and B. Kågström, “An hierarchical approach for performance analysis of scalapack-based routines using the distributed linear algebra machine,” in *Applied Parallel Computing Industrial Computation and Optimization*, ser. Lecture Notes in Computer Science, J. Waśniewski, J. Dongarra, K. Madsen, and D. Olesen, Eds. Springer Berlin Heidelberg, 1996, vol. 1184, pp. 186–195. [Online]. Available: http://dx.doi.org/10.1007/3-540-62095-8_20
- [4] P. Balaprakash, S. M. Wild, and P. D. Hovland, “An experimental study of global and local search algorithms in empirical performance tuning,” in *Proceedings of the 10th International Meeting on High-Performance Computing for Computational Science (VECPAR 2012)*, July 2012, available at <http://www.mcs.anl.gov/~wild/papers/2012/PBSWPH12.pdf>.
- [5] R. Iakymchuk and P. Bientinesi, “Modeling performance through memory-stalls,” *ACM SIGMETRICS Performance Evaluation Review*, vol. 40, no. 2, 2012, to appear.

- [6] P. J. Mucci, S. Browne, C. Deane, and G. Ho, "Papi: A portable interface to hardware performance counters," in *In Proceedings of the Department of Defense HPCMP Users Group Conference*, 1999, pp. 7–10.
- [7] D. Fabregat-Traver and P. Bientinesi, "Automatic generation of loop-invariants for matrix operations," in *Computational Science and its Applications, International Conference*. Los Alamitos, CA, USA: IEEE Computer Society, 2011, pp. 82–92.
- [8] —, "Knowledge-based automatic generation of partitioned matrix expressions," in *Computer Algebra in Scientific Computing*, ser. Lecture Notes in Computer Science, V. Gerdt, W. Koepf, E. Mayr, and E. Vorozhtsov, Eds., vol. 6885. Springer Berlin / Heidelberg, 2011, pp. 144–157.